

Suppression of horizontal vibrations in high-speed elevators using active shock absorber to assist traditional damping systems

Vibration
suppression of
elevator cars

Yaxing Ren, Ren Li, Xiaoying Ru and Youquan Niu
Sicher Elevator Ltd, Huzhou, China

Received 28 September 2023
Revised 14 December 2023
Accepted 2 January 2024

Abstract

Purpose – This paper aims to design an active shock absorber scheme for use in conjunction with a passive shock absorber to suppress the horizontal vibration of elevator cars in a smaller range and shorter time. The developed active shock absorber will also improve the safety and comfort of passengers driving in ultra-high-speed elevators.

Design/methodology/approach – A six-degree of freedom dynamic model is established according to the position and condition of the car. Then the active shock absorber and disturbance compensation-based adaptive control scheme are designed and simulated in MATLAB/Simulink. The results are analysed and compared with the traditional shock absorber.

Findings – The results show that, compared with traditional spring-based passive damping systems, the designed active shock absorber can reduce vibration displacement by 60%, peak acceleration by 50% and oscillation time by 2/3 and is more robust to different spring stiffness, damping coefficient and load.

Originality/value – The developed active shock absorber and its control algorithm can significantly reduce vibration amplitude and converged time. It can also adjust the damping strength according to the actual load of the elevator car, which is more suitable for high-speed elevators.

Keywords Modelling and simulation, Elevator, Vibration suppression, Active shock absorber

Paper type Research paper

1. Introduction

For high-speed elevators, safety and ride comfort are important considerations for modern, high-quality elevators. However, increasing the lifting speed can bring about serious vibration problems, making passengers feel uncomfortable and physiologically fatigued, thus reducing the comfort of passengers and even affecting the service life of the lift as well as the safety of passengers travelling on the lift (Wang *et al.*, 2021; Yang *et al.*, 2014). Previous research results show that when the lift speed exceeds 3 m/s, the transverse vibration acceleration of the lift car will be significantly greater than that of the low-speed lift (Zhang *et al.*, 2019b). Therefore, how to effectively suppress the horizontal vibration of the car becomes one of the important technical difficulties in the field of high-speed and high-performance lift product development (Okada *et al.*, 1994; Utsunomiya *et al.*, 2006). In the past decades, a lot of research has been carried out on the horizontal vibration of high-speed elevators.

The damping of high-speed elevators is often achieved by developing and installing shock absorbers. Generally, the horizontal vibration of elevators occurs due to the deformation of



© Yaxing Ren, Ren Li, Xiaoying Ru and Youquan Niu. Published in *Journal of Intelligent Manufacturing and Special Equipment*. Published by Emerald Publishing Limited. This article is published under the Creative Commons Attribution (CC BY 4.0) licence. Anyone may reproduce, distribute, translate and create derivative works of this article (for both commercial and non-commercial purposes), subject to full attribution to the original publication and authors. The full terms of this licence may be seen at <http://creativecommons.org/licences/by/4.0/legalcode>

Journal of Intelligent
Manufacturing and Special
Equipment
Emerald Publishing Limited
e-ISSN: 2633-660X
p-ISSN: 2633-6596
DOI 10.1108/JIMSE-09-2023-0096

the guide rails. In practice, there are many reasons for horizontal vibration, such as uneven guide rails, abnormal guide rollers, fluctuation of elevator running speed, passenger off-loading and wind shaking (He *et al.*, 2021). The traditional method of vibration damping is to install a spring between the car frame and the guide shoe. This passive shock absorber method is simple in structure, easy to implement, economical and reliable, and the effect is satisfactory when the lifting speed is low because no external energy is required. However, as the speed of the elevator increases, the limitations of passive damping become apparent. For example, it is only applicable to external disturbances with constant frequency or very small changes and can only provide a very small damping force, which makes it difficult to meet the requirements of high-speed elevators. Therefore, the traditional passive damping method is only adapted to the case where the external disturbance input does not change much and cannot provide a large damping force to meet the damping requirements of high-speed elevators (Feng *et al.*, 2009). In the literature, the researchers significantly reduce the horizontal vibration of the car through a series of optimisation steps based on model analysis by reasonably distributing the natural resonance of the elevator car and adding appropriate damping at key points of the car structure (Sissala *et al.*, 1985). Some other researchers reduced horizontal vibration by improving the mechanical characteristics of the elevator (Okada and Nishimura, 1994). In recent years, researchers modelled the dynamics of an elevator and discussed the effect of guide wheel parameters on the car platform acceleration and relative displacement of the guide wheel and car (Fu *et al.*, 2005).

The above studies involve the modelling and analysis of horizontal vibration and the study of suppression methods. These suppression techniques are mainly passive methods that cannot cope with the increase in lifting speed. In contrast, active damping techniques have become a new way to solve elevator vibration with their good effect and adaptability (Noguchi *et al.*, 2011). Typical active shock absorbers include an electromagnetic guide shoe, an electromagnetic damper and an active hydraulic guide shoe (Funai *et al.*, 2004; Mutoh *et al.*, 1999; Utsunomiya, 2001). The semi-active vibration reduction device does not directly output the control force but controls the damping force by changing the damping value, which results in lower energy consumption and stronger anti-interference ability (Wang *et al.*, 2023). The semi-active and active vibration reduction have stronger anti-interference capability and are suitable for the high-speed elevator. Therefore, the vibration modelling and analysis of high-speed elevators provide a basis for the study of vibration damping methods and the development of shock absorbers. However, there are many linear or nonlinear elastic elements in the vibration damping system of a high-speed elevator, and if the design parameters are not selected properly, the high-speed elevator may vibrate violently. The human perception of vibration is not only related to the intensity of vibration but also to the frequency and direction of vibration. The traditional elevator design process has a large degree of randomness in the selection of elastic elements in the guide system. The selection is mainly based on the size of the rolling guide shoe, the width of the wheel and the width of the guide rail. In the literature, the researchers proposed an active damping control method for ultra-high-speed elevators that suppresses vibration by generating the magnetic force required for suppression only when the car frame generates vibration (Mutoh *et al.*, 1999). Apart from that, some researchers have proposed a vibration suppression strategy that uses car acceleration feedback compensation to improve the ride comfort of the elevator (Kang and Sul, 2000). Another study proposed a new control device to suppress horizontal vibration in an elevator car (Nakano *et al.*, 2011). The device consists of two rotating motors with eccentric masses that reduce vibration without generating unwanted vertical vibration. In a recent study, researchers established a horizontal vibration dynamics model for the car of a high-speed elevator by considering the relationship between the lateral force and overturning moment and the horizontal displacement, the deflection angular displacement and the rated velocity (Liu *et al.*, 2019).

However, installing an active control system on each guide shoe would make the shock absorbers numerous and costly. Another problem is that it takes a long time to adjust many parameters of the controller. The control algorithms applied in the above studies are not self-learning for the random excitations of the car system and are slightly less effective. A study analyses the vibration of the elevator from the guide shoe and provides a design idea that can effectively reduce the static horizontal vibration (Utsunomiya, 2001). Another study developed a lift car-slide-guide-coupled lateral vibration model (Guo *et al.*, 2008). Apart from that, some researchers derived the deterministic part and random part of the acceleration response expression based on the ingress theory and analysed the lateral vibration acceleration response at the observation point (Wang *et al.*, 2017). The above studies suppressed the horizontal vibration of high-speed elevators to a certain extent but ignored the difference between the vibration response of the car and the car frame in the actual operation of high-speed elevators. In addition, these did not consider the variation of system parameters (Qiu *et al.*, 2020). A study used operational modal analysis to identify the modal parameters of the elevator car and then estimated the stiffness parameters of the elevator car from these parameters (Kobayashi *et al.*, 2008). Some researchers developed a nonlinear model of a rolling guide shoe and analysed the horizontal vibration response under parameter variations and guideway unevenness (Zhang *et al.*, 2019a; Zhang *et al.*, 2018). In their following study, a BP neural network-based PID controller is designed to control the horizontal vibration of a high-speed elevator to deal with the uncertainty of external excitation in the car system (Zhang *et al.*, 2019b). Some researchers studied the active control strategy of horizontal vibration suppression of high-speed elevator based on linear matrix inequality and reduced the horizontal vibration acceleration of the car system (Cao *et al.*, 2020). In addition, some studies incorporate the sky-hoop damping control strategy into the high-speed elevators structure and adopt a sparrow search algorithm to optimise the parameters to reduce the lateral vibration (Su *et al.*, 2023).

Although the control algorithm can perform intelligent processing such as self-learning and memory for random excitations, it requires a large amount of data for network training to ensure the accuracy of the control. At the same time, due to the black-box nature of the artificial intelligence algorithm, it is not possible to give a clear reasoning basis for its outputs or to apply existing expert knowledge and experience. Therefore, there is a need to develop an active electronic vibration damping device and controller with a simple structure and a good robustness effect to control the horizontal vibration amplitude of the car within a smaller range and to be able to eliminate the vibration quickly. It will also improve the safety and comfort of the passengers when travelling in the ultra-high-speed elevators.

2. Mathematical model of elevator car system

In this section, the elevator car system is modelled based on structural dynamics. The dynamic characteristics of each component in horizontal vibration are obtained from the analytical model. The problem of elevator vibration mainly affects the comfort of the passengers in the car when travelling. When considering the perception of human vibration frequencies, most studies have focused on the low-frequency transverse vibration of the car. The main factors causing transverse vibration in the car are the unevenness of the guideway as well as curvature of the guideway surface and gaps at joints.

An operating elevator is a moving body that exists in six degree of freedom (6DOF), and its degrees of freedom of motion can include up and down, left and right, front and rear directions as well as parallel motion and rotation and torsion around the axis. A commonly used method is to establish a coordinate system to build the dynamical equations with the centre of mass of the elevator as the origin of the coordinates (Utsunomiya *et al.*, 2006).

The motion of the car can be decomposed into the parallel motion of the car's centre of mass and the rotational motion around the centre of mass, and the corresponding state models are represented by the position and attitude equations of the car, respectively. The parallel motion of the centre of mass of the car is represented by the displacement vector at the origin of the linked coordinate system in the inertial coordinate system as follows:

$$\frac{P_1}{\rho} + gz_1 + \frac{v_1^2}{2} = \frac{P_2}{\rho} + gz_2 + \frac{v_2^2}{2} + h_f + \int_s \frac{\partial v}{\partial t} ds \quad (1)$$

In the inertial coordinate system, a system of translational equations is established for the elevator car, and the kinetic equation for the position of the car can be obtained as:

$$\begin{cases} (m_c + \Delta m)\ddot{x} = F_x + \Delta F_x \\ (m_c + \Delta m)\ddot{y} = F_y + \Delta F_y \\ (m_c + \Delta m)\ddot{z} = F_z + \Delta F_z \end{cases} \quad (2)$$

where F_x , F_y , and F_z are the control forces applied along the x , y and z axes, respectively, and ΔF_x , ΔF_y and ΔF_z are the external interference forces along the x , y and z axes, respectively.

The rotational dynamic characteristics of the car are described by the angular coordinates \mathbf{H} . The state quantities are represented by the angles α , β and θ of the rotation of the elevator car around the x , y and z axes of the coordinate system:

$$\mathbf{H} = [\alpha \quad \beta \quad \theta]^T \quad (3)$$

Let the angular velocity of the car relative to the centre of mass be expressed in the coordinate system as:

$$\boldsymbol{\omega} = [\omega_{x'} \quad \omega_{y'} \quad \omega_{z'}]^T \quad (4)$$

Establish the kinematic equations of the elevator car as follows:

$$\boldsymbol{\omega} = \begin{bmatrix} \cos \beta \cos \theta & \sin \theta & 0 \\ -\cos \beta \sin \theta & \cos \theta & 0 \\ \sin \beta & 0 & 1 \end{bmatrix} \begin{bmatrix} \dot{\alpha} \\ \dot{\beta} \\ \dot{\theta} \end{bmatrix} \quad (5)$$

Since the rotation angle of the car itself is very small, it is assumed that:

$$\sin \gamma \approx \gamma, \cos \gamma \approx 1, \text{ where } \gamma = \alpha, \beta, \theta \quad (6)$$

Then the following equation can be obtained:

$$\begin{bmatrix} \dot{\alpha} \\ \dot{\beta} \\ \dot{\theta} \end{bmatrix} = \begin{bmatrix} 1 & -\theta & 0 \\ \theta & 1 & 0 \\ \beta & \theta\beta & 1 \end{bmatrix} \begin{bmatrix} \omega_{x'} \\ \omega_{y'} \\ \omega_{z'} \end{bmatrix} \quad (7)$$

Remove the quadratic term in the formula, the dynamic equation of the car rotation angle can be written as:

$$\begin{bmatrix} \dot{\alpha} \\ \dot{\beta} \\ \dot{\theta} \end{bmatrix} = \begin{bmatrix} \omega_{x'} - \theta\omega_{y'} \\ \theta\omega_{x'} + \omega_{y'} \\ \beta\omega_{x'} + \omega_{z'} \end{bmatrix} \quad (8)$$

According to rigid body dynamics, the motion of the rigid body around the centre of gravity can be expressed by Euler's equation. Therefore, the dynamic model of the rotation of the car can be written as follows in the continuous coordinate system:

$$\begin{cases} I_{x'} \dot{\omega}_{x'} - (I_{y'} - I_{z'}) \omega_{y'} \omega_{z'} = M_{x'} + \Delta M_{x'} \\ I_{y'} \dot{\omega}_{y'} - (I_{z'} - I_{x'}) \omega_{z'} \omega_{x'} = M_{y'} + \Delta M_{y'} \\ I_{z'} \dot{\omega}_{z'} - (I_{x'} - I_{y'}) \omega_{x'} \omega_{y'} = M_{z'} + \Delta M_{z'} \end{cases} \quad (9)$$

where $M_{x'}$, $M_{y'}$, $M_{z'}$ are the control moments applied along the x' , y' , z' axes, respectively, and $\Delta M_{x'}$, $\Delta M_{y'}$, $\Delta M_{z'}$ are the external disturbing moments along the x' , y' , z' axes, respectively. $I_{x'} = J_{x'} + \Delta J_{x'}$, $I_{y'} = J_{y'} + \Delta J_{y'}$, $I_{z'} = J_{z'} + \Delta J_{z'}$, where $I_{x'}$, $I_{y'}$, $I_{z'}$ are the total rotational inertia of the car and load, $J_{x'}$, $J_{y'}$, $J_{z'}$ are the rotational inertia of the car, $\Delta J_{x'}$, $\Delta J_{y'}$, $\Delta J_{z'}$ are the moments of inertia of the load.

The final differential equation expressing the dynamics of the car can be written as:

$$\begin{cases} \dot{\alpha} = \omega_{x'} - \theta \omega_{y'} \\ \dot{\beta} = \theta \omega_{x'} + \omega_{y'} \\ \dot{\theta} = \beta \omega_{x'} + \omega_{z'} \\ \dot{\omega}_{x'} = \frac{M_{x'} + \Delta M_{x'}}{I_{x'}} + \frac{I_{y'} - I_{z'}}{I_{x'}} \omega_{y'} \omega_{z'} \\ \dot{\omega}_{y'} = \frac{M_{y'} + \Delta M_{y'}}{I_{y'}} + \frac{I_{z'} - I_{x'}}{I_{y'}} \omega_{z'} \omega_{x'} \\ \dot{\omega}_{z'} = \frac{M_{z'} + \Delta M_{z'}}{I_{z'}} + \frac{I_{z'} - I_{y'}}{I_{z'}} \omega_{x'} \omega_{y'} \end{cases} \quad (10)$$

In the actual operation of the elevator, in addition to the conventional dynamic characteristics, the transverse vibration of the car also includes the nonlinear response part of the system, such as the nonlinear stiffness and damping of the rollers and springs, as well as the positional change of the guide rails, the phenomenon of the guide shoe gap, the change of the car load with the passenger's movement and entry and exit and the effect of high-speed and ultra-high-speed elevators on the airflow in the shaft. Strictly speaking, the vibration model of the car should be a time-varying system, but these nonlinear factors will greatly increase the complexity of the system and the difficulty of analysis. Therefore, when modelling the lateral vibration of the car, assumptions are often made so that the system can use a linear model to approximate the true dynamic response of the car's motion.

To simplify the model, following assumptions are made:

- (1) There is a rigid connection between the car and the car frame as a single unit, and the sum of their masses is taken as the main mass of the vibration equation;
- (2) The nonlinear stiffness and damping characteristics of the transverse vibration are simplified to a linear spring-damped system;
- (3) No gap in the guide shoe;

(4) No interference response between different guide shoes;

Based on the above assumptions, the simplified model of the dynamics of the lift car vibrating in the horizontal direction is shown in Figure 1.

The equivalent mechanical model of the horizontal vibration of the car has five degrees of freedom, which are the horizontal displacement x of the total weight of the car and car frame in the X-direction, the horizontal displacement y in the Y-direction, the yaw angle α , pitch angle β and tilting angle θ of the car rotating around its centre of gravity. In addition to this, the horizontal movements of the four rollers with masses of m_1, m_2, m_3 and m_4 along the X-axis are x_1, x_2, x_3 and x_4 , and the horizontal movements along the Y-axis are y_1, y_2, y_3 and y_4 , respectively. According to the free-body diagram analysis, the equation of motion for the transverse vibration of the elevator car in the X- and Y-axis directions can be deduced as follows, respectively:

$$m\ddot{x} = k_e(x + a\theta - x_1) + c_e(\dot{x} + a\dot{\theta} - \dot{x}_1) + k_e(x + b\theta + x_2) + c_e(\dot{x} + b\dot{\theta} + \dot{x}_2) + k_e(x - a\theta - x_3) + c_e(\dot{x} - a\dot{\theta} - \dot{x}_3) + k_e(x - b\theta - x_4) + c_e(\dot{x} - b\dot{\theta} - \dot{x}_4) \quad (11)$$

$$m\ddot{y} = k_e(y - a\beta - y_1 - d\alpha) + c_e(\dot{y} - b\dot{\beta} - \dot{y}_1 - d\dot{\alpha}) + k_e(y - b\beta - y_2 + d\alpha) + c_e(\dot{y} - a\dot{\beta} - \dot{y}_2 + d\dot{\alpha}) + k_e(y + a\beta - y_3 - d\alpha) + c_e(\dot{y} + b\dot{\beta} - \dot{y}_3 - d\dot{\alpha}) + k_e(y + b\beta - y_4 + d\alpha) + c_e(\dot{y} + a\dot{\beta} - \dot{y}_4 + d\dot{\alpha}) \quad (12)$$

The differential equations for the deflection, elevation and inclination angles of the car rotating around its centre of gravity are, respectively:

$$J\ddot{\alpha} = k_e d(y + d\alpha - y_1) + c_e d(\dot{y} + d\dot{\alpha} - \dot{y}_1) + k_e d(y + d\alpha - y_2) + c_e d(\dot{y} + d\dot{\alpha} - \dot{y}_2) - k_e d(y - d\alpha - y_3) - c_e d(\dot{y} - d\dot{\alpha} - \dot{y}_3) - k_e d(y - d\alpha - y_4) - c_e d(\dot{y} - d\dot{\alpha} - \dot{y}_4) \quad (13)$$

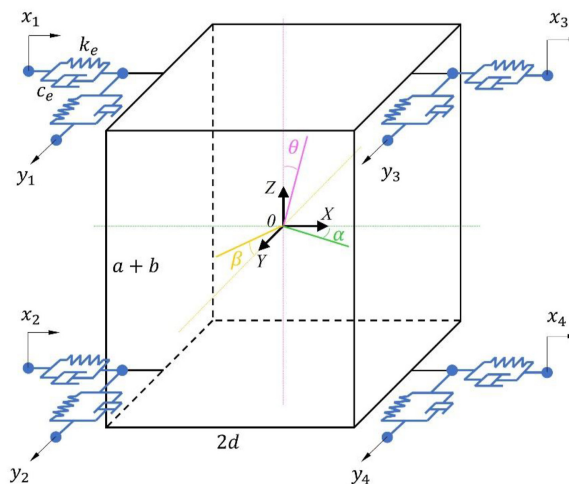


Figure 1.
The dynamic coordinate system of the car

Source(s): Authors' own work

$$J\ddot{\beta} = k_e a(y + a\beta - y_1) + c_e a(\dot{y} + \dot{a}\beta - \dot{y}_1) - k_e b(y - b\beta - y_2) - c_e b(\dot{y} - \dot{b}\beta - \dot{y}_2) \\ + k_e a(y + a\beta - y_3) + c_e a(\dot{y} + \dot{a}\beta - \dot{y}_3) - k_e b(y - b\beta - y_4) - c_e b(\dot{y} - \dot{b}\beta - \dot{y}_4) \quad (14)$$

$$J\ddot{\theta} = k_e a(x + a\theta - x_1) + c_e a(\dot{x} + \dot{a}\theta - \dot{x}_1) - k_e b(x - b\theta - x_2) - c_e b(\dot{x} - \dot{b}\theta - \dot{x}_2) \\ + k_e a(x + a\theta - x_3) + c_e a(\dot{x} + \dot{a}\theta - \dot{x}_3) - k_e b(x - b\theta - x_4) - c_e b(\dot{x} - \dot{b}\theta - \dot{x}_4) \quad (15)$$

The differential equations for the horizontal movement of the four rollers along the X-axis direction and Y-axis direction are:

$$m_1\ddot{x}_1 = k_r(x_1 - x_{c1}) + k_e(x_1 - x - a\theta) + c_e(\dot{x}_1 - \dot{x} - \dot{a}\theta) \quad (16)$$

$$m_2\ddot{x}_2 = k_r(x_2 - x_{c2}) + k_e(x_2 - x + b\theta) + c_e(\dot{x}_2 - \dot{x} + \dot{b}\theta) \quad (17)$$

$$m_3\ddot{x}_3 = k_r(x_3 - x_{c3}) + k_e(x_3 - x - a\theta) + c_e(\dot{x}_3 - \dot{x} - \dot{a}\theta) \quad (18)$$

$$m_4\ddot{x}_4 = k_r(x_4 - x_{c4}) + k_e(x_4 - x + b\theta) + c_e(\dot{x}_4 - \dot{x} + \dot{b}\theta) \quad (19)$$

$$m_1\ddot{y}_1 = k_r(y_1 - y_{c1}) + k_e(y_1 - y - a\beta + d\alpha) + c_e(\dot{y}_1 - \dot{y} - \dot{a}\beta + d\dot{\alpha}) \quad (20)$$

$$m_2\ddot{y}_2 = k_r(y_2 - y_{c2}) + k_e(y_2 - y + a\beta + d\alpha) + c_e(\dot{y}_2 - \dot{y} + \dot{a}\beta + d\dot{\alpha}) \quad (21)$$

$$m_3\ddot{y}_3 = k_r(y_3 - y_{c3}) + k_e(y_3 - y - a\beta - d\alpha) + c_e(\dot{y}_3 - \dot{y} - \dot{a}\beta - d\dot{\alpha}) \quad (22)$$

$$m_4\ddot{y}_4 = k_r(y_4 - y_{c4}) + k_e(y_4 - y + a\beta - d\alpha) + c_e(\dot{y}_4 - \dot{y} + \dot{a}\beta - d\dot{\alpha}) \quad (23)$$

where m is the total mass of the car and the car frame; J is the total rotational inertia of the car and the car frame; a and b denote the vertical distance from the centre of gravity of the car to the centres of the guide shoe at the top and the bottom, respectively; d denotes the horizontal distance from the centre of gravity of the car to the left and right guide shoes; k_e and c_e denote the equivalent spring stiffness and damping, respectively; x and x_1, x_2, x_3, x_4 denote the horizontal displacements of the centre of gravity of the car and the four rollers in the X-axis direction, respectively; y and y_1, y_2, y_3, y_4 denote the horizontal displacements of the centre of mass of the car and the four rollers in the Y-axis direction, respectively; $x_{c1}, x_{c2}, x_{c3}, x_{c4}$ denote the relative displacements of the guideway in the X-axis direction to the four rollers, respectively. $y_{c1}, y_{c2}, y_{c3}, y_{c4}$ represent the relative displacement excitation of the guideway in the Y-axis direction for the four rollers, respectively.

3. Active damping guide shoe design

Among the possible options for an active shock absorber are hydraulic and electromagnetic dampers. Electromagnetic dampers possess high reliability and better dynamic performance as well as a smaller size, lighter weight and lower cost compared to hydraulic dampers (Yang *et al.*, 2017). Moreover, hydraulic/pneumatic damping solutions are costly, bulky and energy-intensive. Electromagnetic dampers, on the other hand, have the advantage of energy recovery in addition to good vibration damping performance (Fang *et al.*, 2013; Li, 2012). The combination of a linear motor or rotary motor plus a rack and pinion is usually chosen as the active electromagnetic damper.

Since the linear motor and passive spring damping work simultaneously, the damping effect can be improved by hybrid electromagnetic damping. The active damping guide shoe of the car based on electromagnetic damping method is shown in Figure 2. The red part represents the linear motor operating in parallel with the spring passive damping, which provides electromagnetic force f_1 to improve the damping effect when the car vibrates.

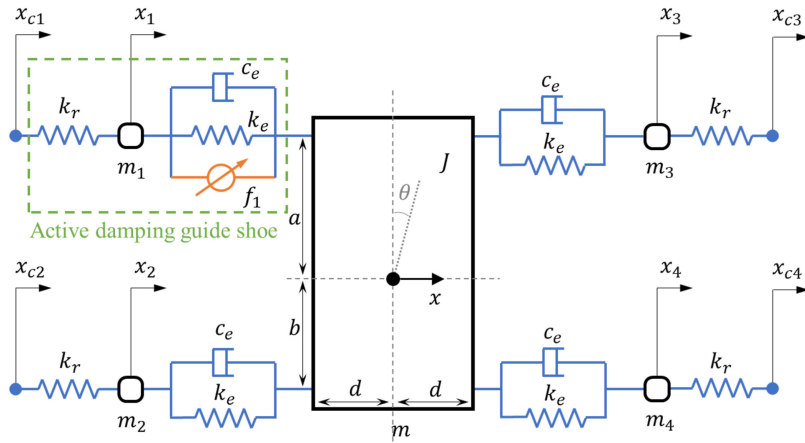


Figure 2. Car electronic vibration reduction system based on active vibration reduction equipment

Source(s): Authors' own work

The current of the electromagnetic damper is regulated by a controller, which usually executes the control algorithm through electronic devices. The electric active damping algorithm design should take into account that when the vibration occurs, the amplitude of the car's vibration should be reduced quickly so that it can converge to 0 in the shortest possible time. Based on this, this paper uses the PD control to regulate the stress generated by the active shock absorber to eliminate the car's vibration quickly. The control block diagram of the active damping system of the car elevator is shown in Figure 3.

The control obtains the rate of change dx of the lateral vibration of the car from the sensors and calculates the optimum stress to be compensated by the PD controller. As a passive damper based on a conventional spring mechanism is also used, the amount of disturbance needs to be compensated out of the calculated optimum compensating stress and the resulting difference is sent to the current management of the linear motor to regulate the motor output electromagnetically f , which assists the car to reduce the transverse vibration to 0 as soon as possible.

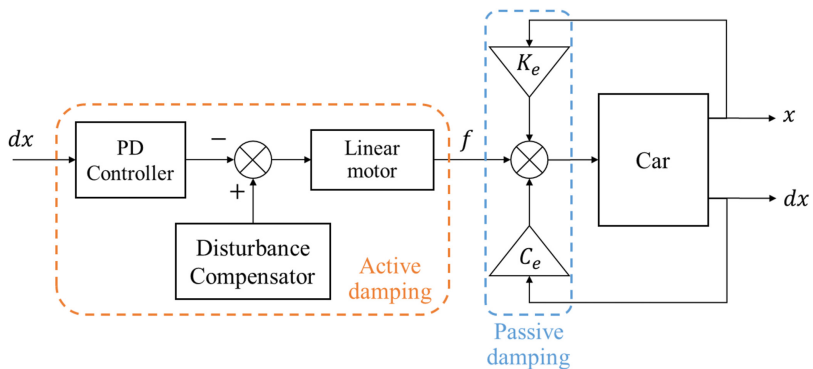


Figure 3. Control block diagram of an active shock absorber

Source(s): Authors' own work

4. Results and discussion

4.1 Simulation result of car vibration

In order to further analyse the dynamic process of lateral vibration of the car, the mathematical model of car vibration was simulated using simulation software, MATLAB/Simulink. The simulation software was used to build a mathematical model of the 6DOF car dynamics and to simulate its vibration state under different environments and excitations. The model parameters of the car in simulation are set as shown in Table 1. The method of analysing the impulse response is chosen to verify the dynamic response of the car vibration, i.e. to give an impulse excitation to a single guide shoe, both in the X-axis direction and in the Y-axis direction, and to observe the vibration response of the car in the time domain at the subsequent time after the guide shoe has been excited by the impulse.

As can be seen from Figure 4, after the guide shoe is excited by a pulse with an amplitude of 1 cm in the X-axis direction, the car starts to vibrate greatly at its intrinsic frequency of about 1 Hz, with the maximum displacement of the car in the X-axis direction of 5.5 mm and the maximum tilting angle of the car of about 0.002° . When the impulse excitation of the guide shoe ends, the amplitude of the car vibration gradually converges to 0 under the effect of spring stiffness and damping, and the damping time is about 20 s under the original damping system. As the guide shoe is only excited by impulses in the X-axis direction in this test, the displacement of the car in the Y-axis direction as well as the yaw and pitch angles of the car rotation remain unchanged.

In order to verify the vibration response of the car after the guide shoe is excited by a pulse in the Y-direction, Figure 5 shows the vibration response of the car after the guide shoe is excited by a pulse with an amplitude of 1 cm in the Y-direction. Similar to the response of the car after the pulse excitation in the X-axis direction, the maximum horizontal displacement of the car in the Y-direction after the pulse excitation in the Y-axis direction is about 12 mm and converges to 0 after 20 s. However, due to the influence of the position of the guide shoe, there is a big difference in the vibration response of the car's yaw and pitch angles. The car pitch angle converges to 0 in only 5 s under the same boot impulse excitation, whereas the car yaw angle takes much longer to converge to 0, in this case after about 30 s. Similarly, since the boot excitation in this case occurs only in the Y-axis direction, the X-direction displacement as well as the car tilting angle are kept constant.

In order to investigate the interaction between the horizontal vibrations of the car in the X- and Y-axis directions, the same guide shoe is excited by an impulse in both the X- and Y-axis directions, and the overall vibration response of the car is shown in Figure 6. Comparing Figure 6 with Figures 4 and 5, it can be seen that there is no significant difference between the horizontal vibration of the car in the X-axis direction only and the impulsive vibration occurring in both the X- and Y-axis directions at the same time. It can therefore be

Parameters	Symbol	Value	Unit
Car mass	m	2,384	kg
Car moment of inertia	J	7,048	$\text{kg} \cdot \text{m}^2$
Distance from centre of gravity to top of the car	a	2.5	m
Distance from centre of gravity to bottom of the car	b	2.1	m
Distance from centre of gravity to side of the car	d	1.5	m
Equivalent spring stiffness	k_e	4×10^2	N/m
Equivalent damping coefficient	c_e	4×10^2	$\text{N} \cdot \text{s}/\text{m}$
Mass of guide wheel	$m_1 \sim m_4$	5	kg

Source(s): Authors' own work

Table 1.
Car simulation model
parameters

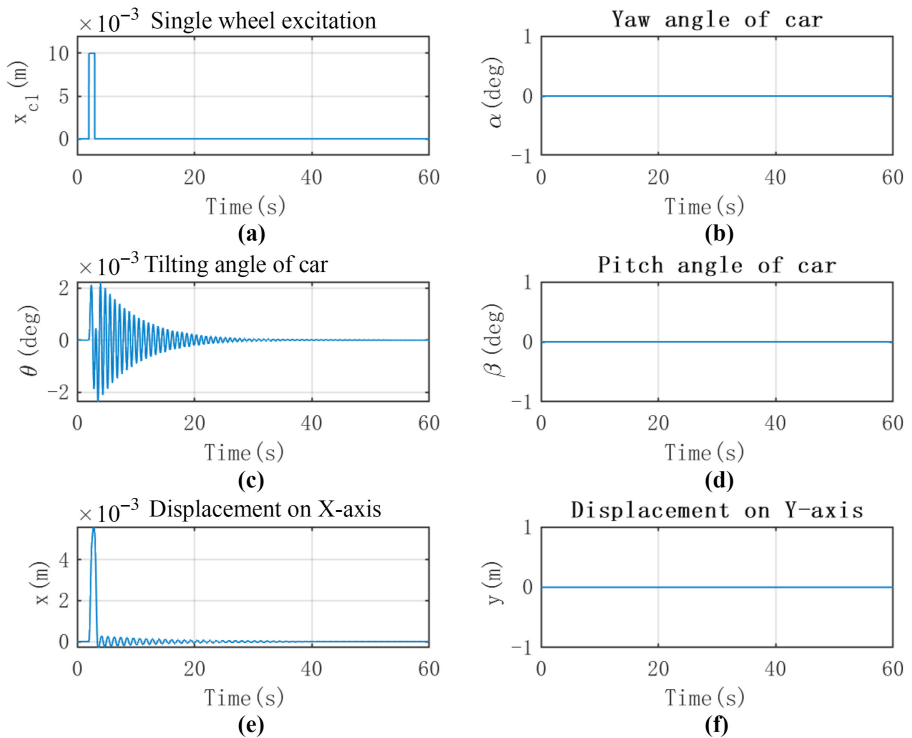


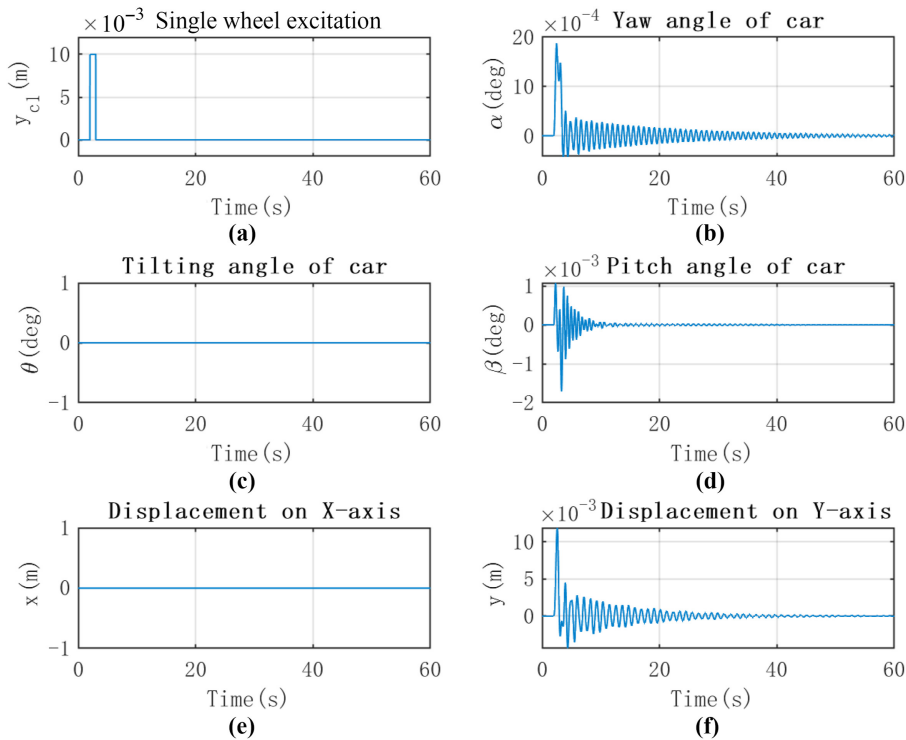
Figure 4. The vibration response of the car under the excitation of a single guide shoe in the X-direction: (a) guide wheel excitation, (b) yaw angle, (c) tilting angle, (d) pitch angle, (e) displacement in the X-direction and (f) displacement in the Y-direction

Source(s): Authors' own work

determined that the vibration responses of the car in the X- and Y-axis directions are orthogonal and can be analysed independently. Therefore, it is possible to analyse the X-axis and Y-axis vibrations independently of each other without having to design a damping scheme for the interaction between these two.

4.2 Car vibration analysis

The vibration response of the car is related to the stiffness and damping coefficient of the active damping system. Also, different passenger loads have a significant effect on the response to the car vibration. Figure 7 illustrates the maximum displacement in the X- and Y-axis directions of a car with a common vibration damping system for different loads in relation to stiffness. As shown in Figure 7 (a), the blue line in the figure indicates the maximum displacement in the X-axis direction of the car vibrating under impulse-guided shoe excitation versus the stiffness when the elevator is not loaded. When the stiffness of the damping system is 5×10^4 N/m, the maximum displacement of the car in X-direction is the smallest, which is about 5 mm; when the stiffness of the damping system increases or decreases, the maximum displacement of the car in X-direction increases under the same impulse excitation, and it reaches the highest value of about 7.5 mm, which is 50% more than the minimum value when the stiffness is 1×10^4 N/m or 9×10^4 N/m. The maximum displacement of the car is about 7.5 mm, which is 50% higher than the minimum value.



Source(s): Authors' own work

Figure 5. Car vibration response under Y-direction excitation of single guide shoe: (a) guide wheel excitation, (b) car deflection, (c) car inclination, (d) car elevation, (e) displacement in the X-direction and (f) displacement in the Y-direction

In addition to the maximum displacement, the vibration response metrics of the car in the X-direction include the X-direction acceleration and accumulated displacement, as shown in Figure 7 (c) and (e). As can be seen from the results in the figure, the X-direction acceleration increases with the increase in stiffness and decreases with the increase in load, indicating that the greater the stiffness, the greater the lateral thrust felt by the passengers under the horizontal excitation of the guide shoe. The X-direction accumulated displacement represents the overall period of the vibration. It can be seen that the trend of change is similar to that of the maximum displacement. It can be seen that the trend is similar to the maximum displacement, with smaller accumulated displacements for small loads and larger accumulated displacements for large loads at lower stiffnesses and vice versa.

Under the excitation of the guide wheel in the Y-direction, the maximum displacement, acceleration and accumulated displacement of the car in the Y-direction with respect to the stiffness and load are shown in Figure 7 (b), (d) and (f), respectively.

In addition to the elastic stiffness, the damping coefficient of the damping system also has a great influence on the car's vibration response. The same as stiffness, the maximum displacement, acceleration and accumulated displacement of the car in the X- and Y-directions with respect to the damping coefficient and load under the same excitation are shown in Figure 8. It can be seen that when the damping coefficient increases, the displacement and acceleration of the car decrease significantly. At the same time, when the load is increased, the maximum displacement and accumulated displacement of the car rise significantly, but the acceleration decreases significantly.

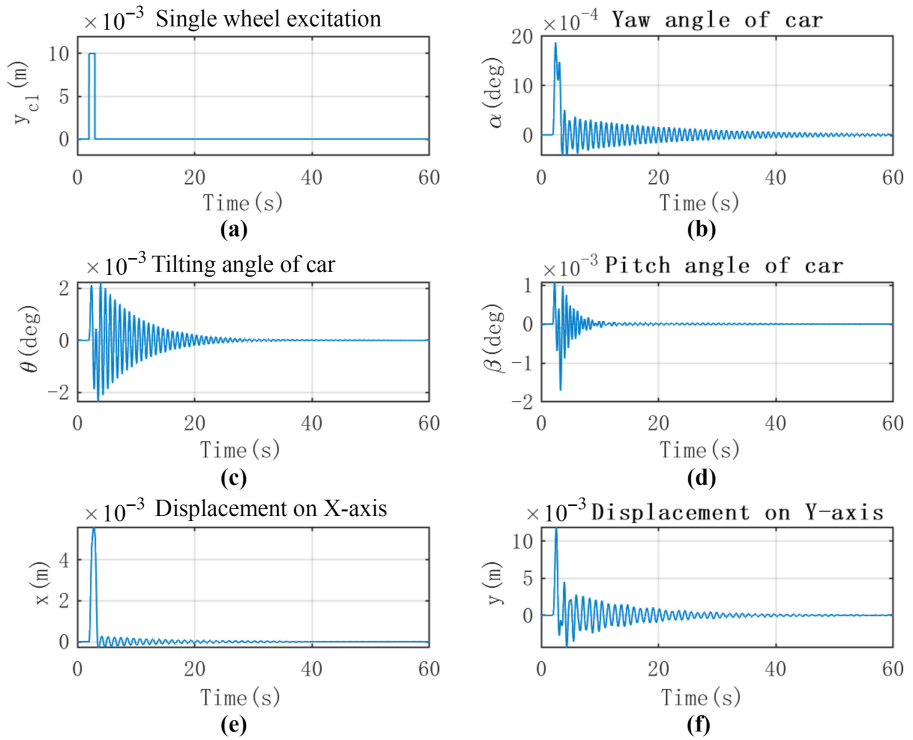


Figure 6. The vibration response of the car under the excitation of the X- and the Y-direction of a single guide shoe: (a) guide wheel excitation, (b) car deflection, (c) car inclination, (d) car elevation, (e) displacement in the X-direction and (f) displacement in the Y-direction

Source(s): Authors' own work

4.3 Comparison of traditional and active shock absorbers

In this section, the performance of the developed active shock absorber and its vibration control algorithm is simulated and compared with the traditional vibration damping system. The two main modes, step response and impulse response, of the guide shoe excitation are verified. The results are shown in [Figures 9 and 10](#), respectively.

When the guide shoe is subjected to step excitation, there is a significant displacement of the car in both X- and Y-directions. For the X-direction displacement, the car vibration of the active shock absorber converges and reaches a steady state faster than the traditional passive damping system, reducing the horizontal vibrating period by more than 2/3. For displacements in the Y-direction, the vibration amplitude of the actively damped car is significantly reduced, in addition to halving the maximum displacement. Due to the different layout of the damping systems in the X- and Y-directions, the car deflection and elevation angles are more difficult to converge than the car tilting angle. From the results, an active shock absorber is less effective in suppressing car vibration in its yaw angle and pitch angle, but very effective in suppressing car vibration in its tilting angle.

Under impulse excitation, which is equivalent to two-step excitations in a short period of time, it has a greater impact on the vibration response of the car. After the guide shoe is excited by the impulse, the maximum displacement of the car based on the active shock absorber is significantly reduced in both the X- and Y-directions due to the compensation of the active damping system. The vibration is therefore able to attenuate quickly after the excitation. In addition to the displacement of the car, the elimination of vibration on its tilting

Vibration suppression of elevator cars

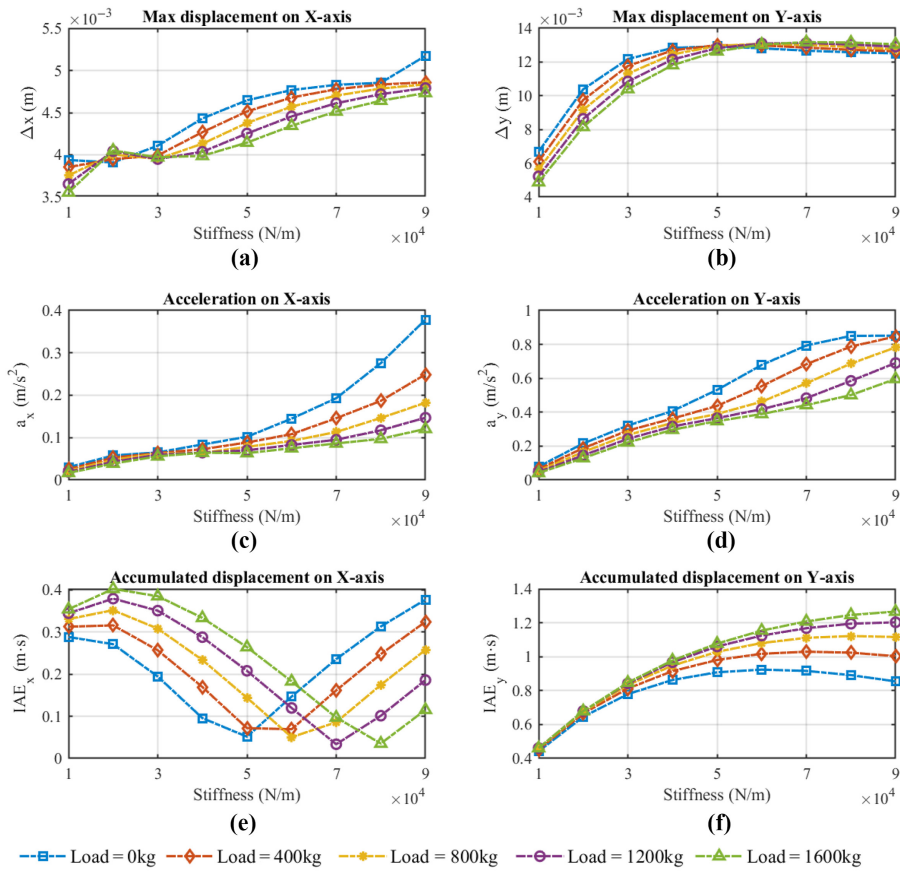


Figure 7. The relationship between the maximum displacement and the elastic stiffness of the car under different loads using traditional shock absorber: (a) maximum displacement in X-direction, (b) maximum displacement in Y-direction, (c) acceleration in X-direction, (d) acceleration in Y-direction, (e) cumulative displacement in X-direction and (f) cumulative displacement in Y-direction

Source(s): Authors' own work

angle is significantly improved. The attenuation of the yaw and pitch angles is not only significantly improved but can also be effectively controlled.

In order to quantify the improvement of the active shock absorber, Table 2 expressed the maximum error and integrated absolute error (IAE) of vibration suppression in terms of the displacement of the x -axis and y -axis, yaw, tilt and pitch angle. From the table, it can be seen that the displacement of vibration has been suppressed by 22.7 and 42.9% in maximum and 52.1 and 77.9% in IAE in the x -axis and y -axis, respectively. The rotational angles of the car system have been reduced by 1/3 in tilt and pitch, while the yaw angle remains the same in maximum error. From the results, it can be seen that after using an active shock absorber, only the IAE of pitch angle has increased compared to a traditional shock absorber, while all other vibration variables have significantly decreased.

4.4 Impact of changing car parameters on active shock absorber

When the stiffness, damping coefficient and passenger load of the car system are varying, the vibration response of the car in the time series will be varied accordingly. In the same way as the validation method for general vibration damping, the maximum displacement,

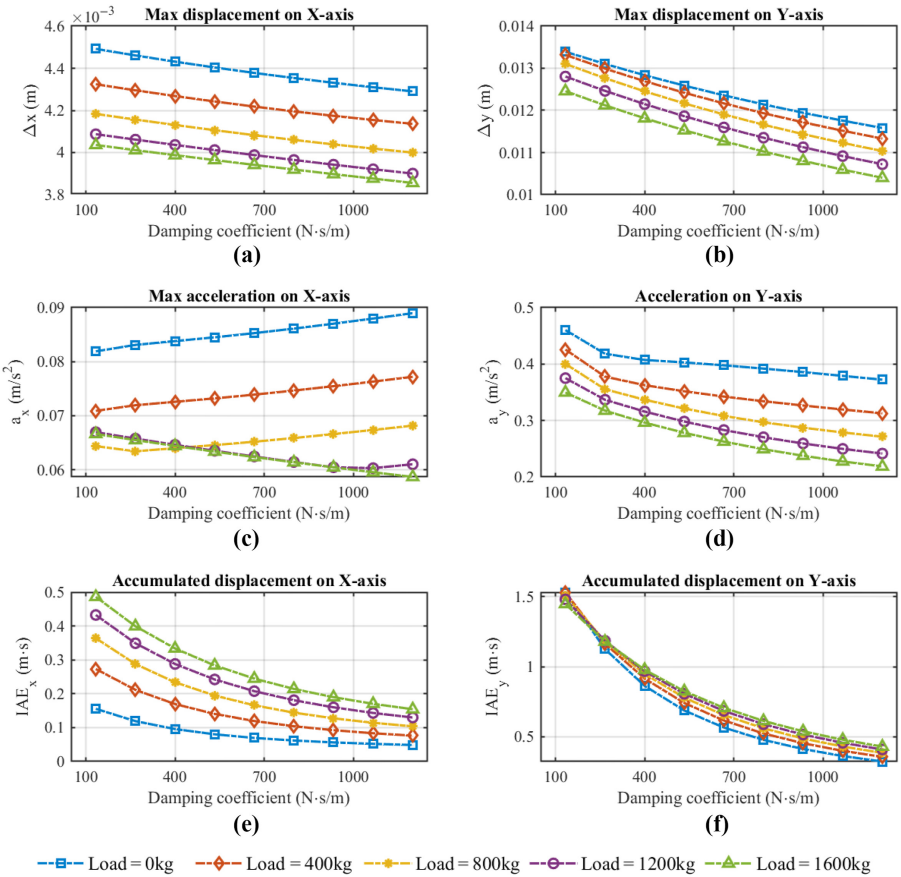


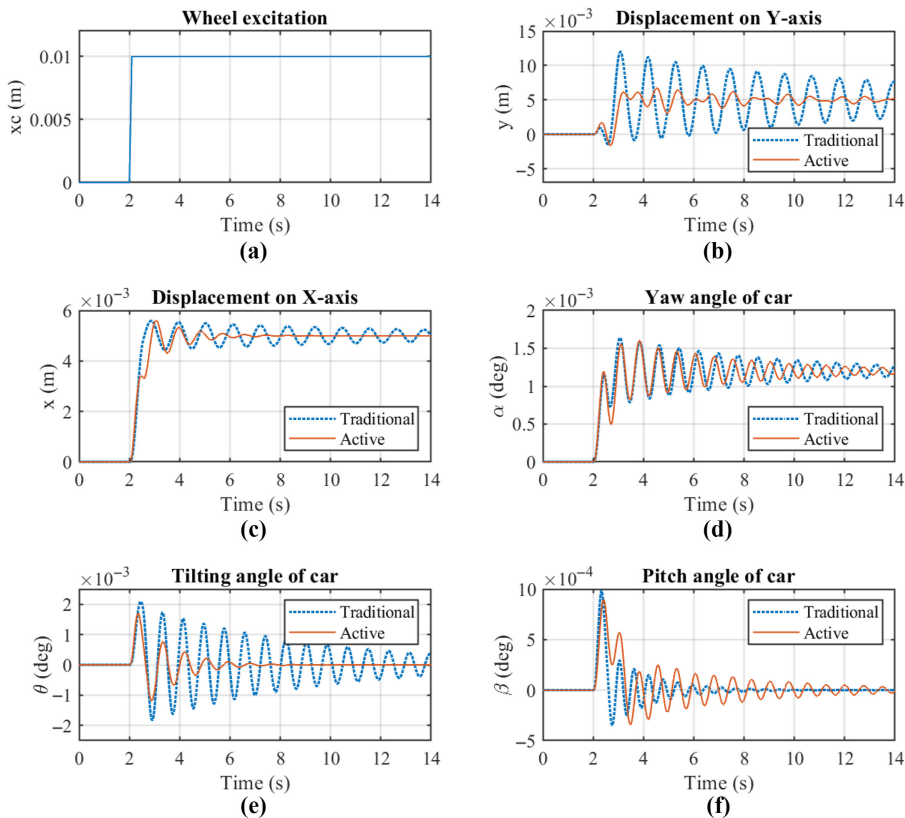
Figure 8. The relationship between the maximum displacement and the damping coefficient of the car under different loads using traditional shock absorber: (a) maximum displacement in X-direction, (b) maximum displacement in Y-direction, (c) acceleration in X-direction, (d) acceleration in Y-direction, (e) cumulative displacement in X-direction and (f) cumulative displacement in Y-direction

Source(s): Authors' own work

acceleration and accumulated displacement in the X- and Y-directions were chosen as indicators of car vibration for the validation of the active vibration damping system. The relationship between the displacement and the stiffness of the car with an active shock absorber at different loads is shown in Figure 11 and the relationship with the damping coefficient is shown in Figure 12.

Comparing Figures 7 and 11, it can be seen that, as the proposed scheme actively compensates for the stress of the car vibration, the amplitude and duration of the car vibration based on the active shock absorber are greatly reduced under different stiffnesses of the damping system, which effectively improves the vibration damping performance of the car. From the data, the maximum X-direction displacement of the car based on normal damping is in the range of 3.5 mm–5.5 mm under the same impulse excitation, while the maximum X-direction displacement of the car based on active damping is controlled in the range of 2.6 mm–3.4 mm. At the same time, the acceleration in the X-direction was reduced by more than 50% than traditional damping and the accumulated displacement was reduced by 75%–90%. The vibration control in the Y-direction was not as effective as the damping in the X-direction, with the maximum displacement and acceleration reduced by about 20%. The

Vibration suppression of elevator cars



Source(s): Authors' own work

Figure 9. Comparison of vibration response of traditional shock absorber and active shock absorber under step-by-step excitation: (a) guide wheel excitation, (b) car deflection, (c) car inclination, (d) car elevation, (e) displacement in the X-direction and (f) displacement in the Y-direction

accumulated displacement was still reduced by more than 75%, which is a very significant improvement in damping behaviour.

Comparison of Figures 8 and 12 shows that at different damping coefficients of the damping system, the maximum displacement and acceleration of the X-direction of the car based on active damping are close to those of traditional damping. But the accumulated displacement decreases significantly and is obviously reduced significantly by the low damping coefficient of the damping system, up to a maximum reduction of 90%. From the Y-direction vibration damping data, the trend of vibration elimination remains the same when the damping coefficient changes, i.e. the larger the damping coefficient, the lower the maximum displacement, acceleration and accumulated displacement. Numerically, the maximum displacement and acceleration in the Y-direction decreased by 40% and the accumulated displacement decreased by 80%.

It is concluded that the vibration damping effect of the active damping scheme in the X-direction is significantly higher than that in the Y-direction. The enhancement of the vibration damping effect is better under low damping coefficients than under high damping. At the same time, the most suitable stiffness and damping coefficient of the vibration damping system can be determined according to the design load of the elevator and the comfort level, which can maximise the vibration damping performance of the active shock absorber and contribute to the high-end development of elevator products.

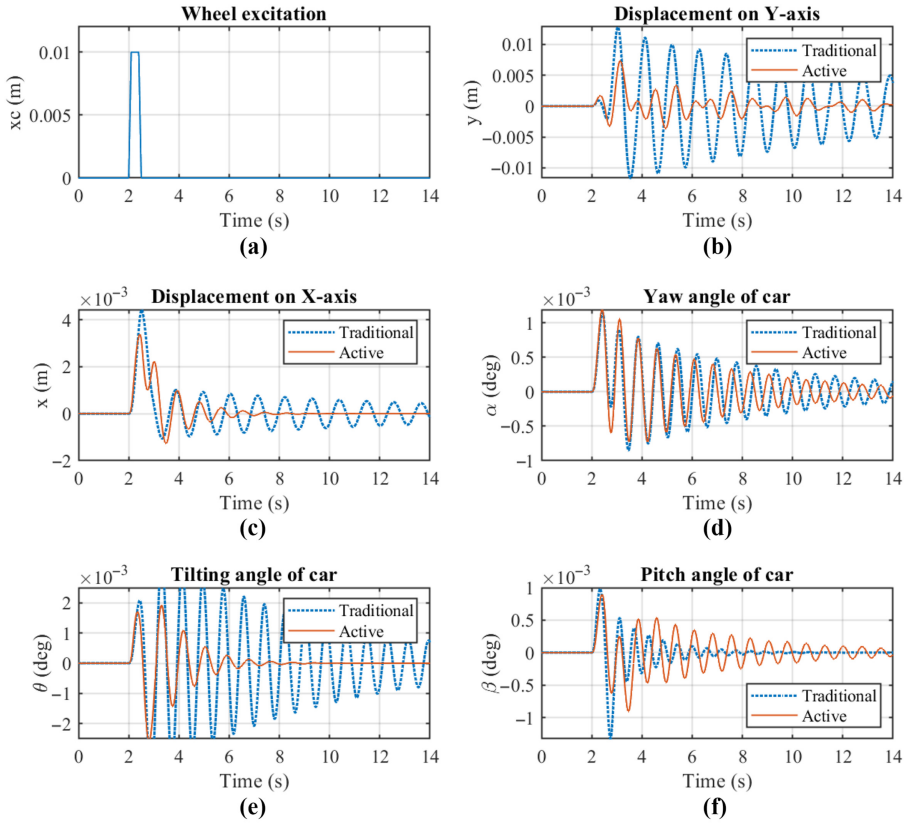


Figure 10. Comparison of vibration response of traditional shock absorption and electronic shock absorption under pulse excitation: (a) guide wheel excitation, (b) car deflection, (c) car inclination, (d) car elevation, (e) displacement in the X-direction and (f) displacement in the Y-direction

Source(s): Authors' own work

Table 2. Comparison of vibration reduction between traditional and active shock absorbers

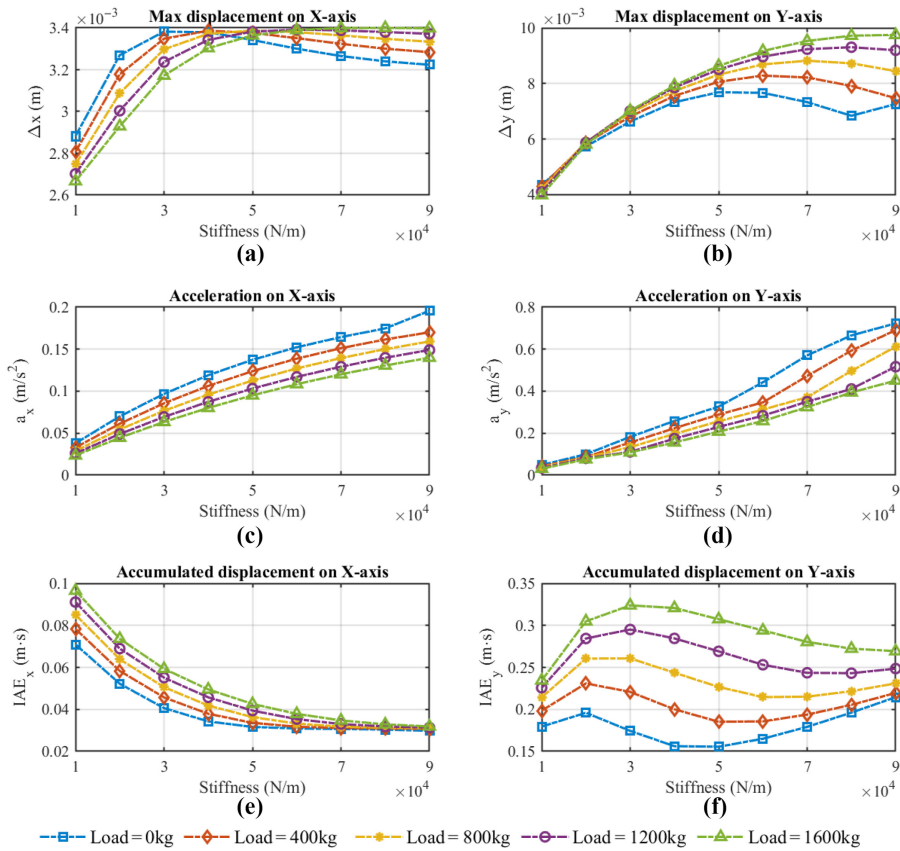
Param	Traditional		Active		Improvement	
	Max err	IAE	Max err	IAE	Max err	IAE
x [m]	0.0044	0.0071	0.0034	0.0034	-22.7%	-52.1%
y [m]	0.0128	0.0589	0.0073	0.013	-42.9%	-77.9%
α [deg]	0.0012	0.0035	0.0012	0.003	0%	-14.3%
β [deg]	0.0013	0.0012	0.0009	0.0023	-30.7%	91.7%
θ [deg]	0.0039	0.0146	0.0026	0.0033	-33.3%	-77.4%

Source(s): Authors' own work

5. Conclusion

In this paper, an active shock absorber and its control system are designed to suppress the horizontal vibration of high-speed elevators. Firstly, based on the motion equation, a 6DOF dynamic model was established according to the position and condition of the car system. Then the scheme based on the traditional passive damping shock absorber is tested and analysed. The amplitude and convergence speed of the lateral displacement and angle changes of the car system under the same excitation were compared between traditional and

Vibration suppression of elevator cars



Source(s): Authors' own work

Figure 11. The relationship between the maximum displacement and elastic stiffness of the car under different loads using active shock absorber: (a) maximum displacement in X-direction, (b) maximum displacement in Y-direction, (c) acceleration in X-direction, (d) acceleration in Y-direction, (e) cumulative displacement in X-direction and (f) cumulative displacement in Y-direction

active shock absorbers. The results show that the designed active shock absorber can maintain the vibration amplitude within a smaller range, reducing the vibration range of the car by 60% and acceleration by 50% in the X-direction and by 20% in the Y-direction. Meanwhile, compared with traditional damping schemes, the active shock absorber can also eliminate vibration faster, reducing horizontal vibration time by more than 2/3. Even if the active shock absorber is only used at one of the four positions where the elevator guide shoe is located, it can still control the horizontal vibration amplitude of the elevator car within a smaller range. At last, this paper tested the car's vibration under different loads, stiffness and damping coefficients to verify that the active shock absorber is more robust than the traditional shock absorber. The results verify that the active shock absorber performs better in adaptation to the elevator's horizontal vibration suppression effect in different scenarios and working conditions.

The novelty of this paper has been summarized as follows:

- (1) The disturbance compensation-based control scheme for the active shock absorber has been designed to adaptively reduce the horizontal vibration of the elevator car system.

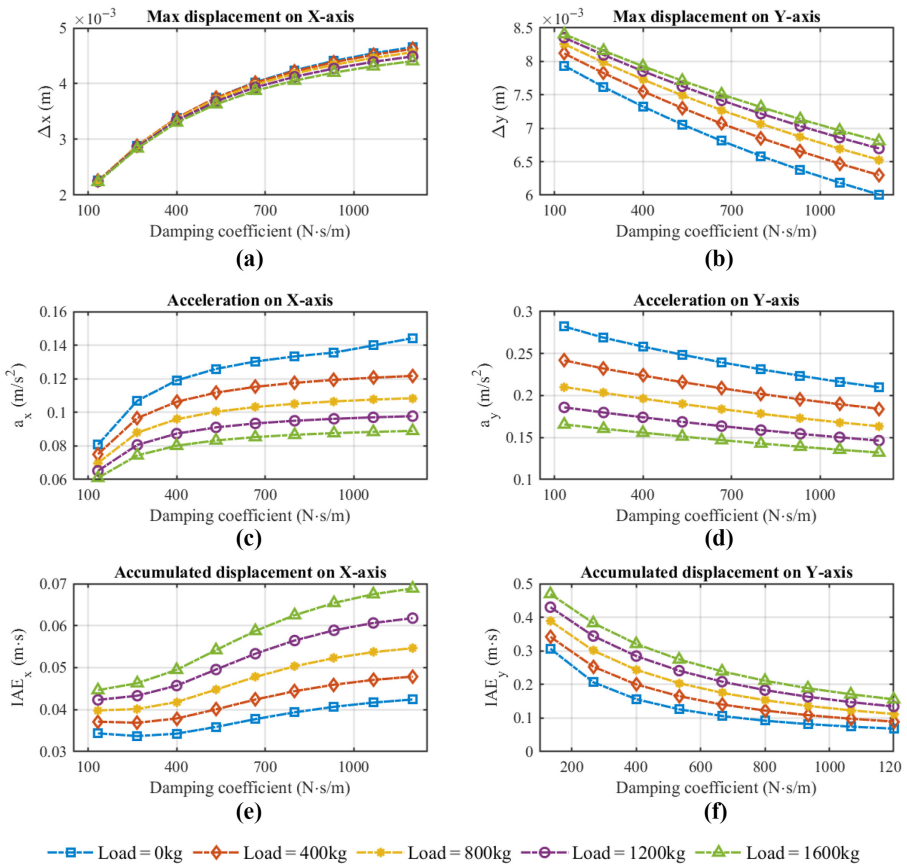


Figure 12. The relationship between the maximum displacement of the car and the damping coefficient under different loads using active shock absorber: (a) maximum displacement in X-direction, (b) maximum displacement in Y-direction, (c) acceleration in X-direction, (d) acceleration in Y-direction, (e) cumulative displacement in X-direction and (f) cumulative displacement in Y-direction

Source(s): Authors' own work

- (2) The design of the active shock absorber is to add an active damping device on the basis of traditional passive damping systems, which is not only easier to implement but also does not affect the original damping design.
- (3) Equip an active damping device only in one of the four guide shoe positions to verify whether good car vibration suppression performance can be achieved while saving costs by using fewer active shock absorbers in the elevator car system.

Therefore, the developed active shock absorber and its control algorithm are verified to have the ability to adjust the damping strength according to the actual passenger load inside the car to reduce the horizontal vibration of the elevator, making it more suitable for use in high-speed elevators.

References

Cao, S., He, Q., Zhang, R. and Cong, D. (2020), "Active control strategy of high-speed elevator horizontal vibration based on LMI optimization", *CEAI*, Vol. 22.

- Fang, Z., Guo, X., Xu, L. and Zhang, H. (2013), "Experimental study of damping and energy regeneration characteristics of a hydraulic electromagnetic shock absorber", *Advances in Mechanical Engineering*, Vol. 5 No. 2, pp. 99-107, doi: [10.1155/2013/943528](https://doi.org/10.1155/2013/943528).
- Feng, Y., Zhang, J. and Zhao, Y. (2009), "Modeling and robust control of horizontal vibrations for high-speed elevator", *Journal of Vibration and Control*, Vol. 15 No. 9, pp. 1375-1396, doi: [10.1177/1077546308096102](https://doi.org/10.1177/1077546308096102).
- Fu, W., Liao, X. and Zhu, C. (2005), "Structural optimization to suppress elevator horizontal vibration using virtual prototype", *Journal of System Simulation*, Vol. 17 No. 6, pp. 1500-1504.
- Funai, K., Katayama, H., Higaki, J., Utsonomiya, K. and Nakashima, S. (2004), "The development of active vibration damper for super high-speed elevators", *Lift Report*, Vol. 5 No. 1, pp. 22-37.
- Guo, K., Li, H. and Meng, G. (2008), "Modeling and simulation of vibration for slide guide system in an elevator", *Journal of Vibration and Shock*, Vol. 158 No. 1, p. 93.
- He, Q., Zhang, P., Cao, S., Zhang, R. and Zhang, Q. (2021), "Intelligent control of horizontal vibration of high-speed elevator based on gas-liquid active guide shoes", *Mechanics and Industry*, Vol. 22, p. 2, doi: [10.1051/meca/2020100](https://doi.org/10.1051/meca/2020100).
- Kang, J.-K. and Sul, S.-K. (2000), "Vertical-vibration control of elevator using estimated car acceleration feedback compensation", *IEEE Transactions on Industrial Electronics*, Vol. 47 No. 1, pp. 91-99, doi: [10.1109/41.824130](https://doi.org/10.1109/41.824130).
- Kobayashi, S., Yoshimura, T., Noguchi, N. and Omiya, A. (2008), "Estimation of dynamic characteristics of an elevator car using operational modal analysis", *Transactions of the Japan Society of Mechanical Engineers, Series C*, Vol. 74 No. 739, pp. 548-553, doi: [10.1299/kikaic.74.548](https://doi.org/10.1299/kikaic.74.548).
- Li, Z. (2012), "Regenerative shock absorbers for energy harvesting from vehicle suspensions", in *State University of New York at Stony Brook*.
- Liu, J., Zhang, R., He, Q. and Zhang, Q. (2019), "Study on horizontal vibration characteristics of high-speed elevator with airflow pressure disturbance and guiding system excitation", *Mechanics and Industry*, Vol. 20 No. 3, p. 305, doi: [10.1051/meca/2019013](https://doi.org/10.1051/meca/2019013).
- Mutoh, N., Kagomiya, K., Kurosawa, T., Konya, M. and Andoh, T. (1999), "Horizontal vibration suppression method suitable for super-high-speed elevators", *Electrical Engineering in Japan*, Vol. 129 No. 1, pp. 59-73, doi: [10.1002/\(sici\)1520-6416\(199910\)129:13.0.co;2-1](https://doi.org/10.1002/(sici)1520-6416(199910)129:13.0.co;2-1).
- Nakano, K., Hayashi, R., Suda, Y., Noguchi, N. and Arakawa, A. (2011), "Active vibration control of an elevator car using two rotary actuators", *Journal of System Design and Dynamics*, Vol. 5 No. 1, pp. 155-163, doi: [10.1299/jsdd.5.155](https://doi.org/10.1299/jsdd.5.155).
- Noguchi, N., Arakawa, A., Miyata, K., Yoshimura, T. and Shin, S. (2011), "Study on active vibration control for high-speed elevators", *Journal of System Design and Dynamics*, Vol. 5 No. 1, pp. 164-179, doi: [10.1299/jsdd.5.164](https://doi.org/10.1299/jsdd.5.164).
- Okada, K. and Nishimura, N. (1994), "Noise and vibration reduction techniques for 750m/min elevators", *Mitsubishi Electric Advance*, Vol. 67, pp. 2-4.
- Okada, K., Sugiyama, Y., Yamazaki, Y. and Tomisawa, M. (1994), "Vibration control of super-high-speed elevators", *Transactions of the Japan Society of Mechanical Engineers*, Vol. 60 No. 579, pp. 3782-3788, doi: [10.1299/kikaic.60.3782](https://doi.org/10.1299/kikaic.60.3782).
- Qiu, L., Wang, Z., Zhang, S., Zhang, L. and Chen, J. (2020), "A vibration-related design parameter optimization method for high-speed elevator horizontal vibration reduction", *Shock and Vibration*, pp. 1-20, doi: [10.1155/2020/1269170](https://doi.org/10.1155/2020/1269170).
- Sissala, M., Heimola, T. and Ojala, M. (1985), "Optimization of lift car vibrational behaviour by modal analysis", *Elevator World*, Vol. 6, pp. 27-31.
- Su, W., Jiang, Y., Yi, C. and Li, S. (2023), "Lateral vibration control strategy of high-speed elevator car based on sparrow search optimization algorithm", *Applied Sciences (Switzerland)*, Vol. 13 No. 18, 10527, doi: [10.3390/app131810527](https://doi.org/10.3390/app131810527).

-
- Utsunomiya, K. (2001), "Active roller guide system for high-speed elevators", *ELEVCON*, pp. 198-205.
- Utsunomiya, K., Okamoto, K., Yumura, T. and Sakuma, Y. (2006), "Vibration control of high-speed elevators taking account of electricity consumption reduction", *Transactions of the Japan Society of Mechanical Engineers C*, Vol. 72 No. 719, pp. 2048-2055, doi: [10.1299/kikaic.72.2048](https://doi.org/10.1299/kikaic.72.2048).
- Wang, C., Zhang, R. and Zhang, Q. (2017), "Analysis of transverse vibration acceleration for a high-speed elevator with random parameter based on perturbation theory", *International Journal of Acoustics and Vibration*, Vol. 22 No. 2, pp. 218-223, doi: [10.20855/ijav.2017.22.2467](https://doi.org/10.20855/ijav.2017.22.2467).
- Wang, H., Zhang, M., Zhang, R. and Liu, L. (2021), "Research on predictive sliding mode control strategy for horizontal vibration of ultra-high-speed elevator car system based on adaptive fuzzy", *Measurement and Control*, Vol. 54 Nos 3-4, pp. 360-373, doi: [10.1177/00202940211003926](https://doi.org/10.1177/00202940211003926).
- Wang, Z., Qiu, L., Zhang, S., Su, G., Zhu, L. and Zhang, X. (2023), "High-speed elevator car system semi-active horizontal vibration reduction method based on the improved particle swarm algorithm", *JVC/Journal of Vibration and Control*, Vol. 29 Nos 13-14, pp. 2921-2934, doi: [10.1177/10775463221089425](https://doi.org/10.1177/10775463221089425).
- Yang, I.H., Jeong, J.E., Jeong, U.C., Kim, J.S. and Oh, J.E. (2014), "Improvement of noise reduction performance for a high-speed elevator using modified active noise control", *Applied Acoustics*, Vol. 79, pp. 58-68, doi: [10.1016/j.apacoust.2013.10.016](https://doi.org/10.1016/j.apacoust.2013.10.016).
- Yang, S., Kang, Y., Chen, H. and Yuan, J. (2017), *Electromagnetic Nondestructive Testing of Wire Ropes*, Machinery Industry Press, Beijing.
- Zhang, R.-J., Wang, C. and Zhang, Q. (2018), "Response analysis of the composite random vibration of a high-speed elevator considering the nonlinearity of guide shoe", *Journal of the Brazilian Society of Mechanical Sciences and Engineering*, Vol. 40 No. 4, pp. 1-10, doi: [10.1007/s40430-017-0936-0](https://doi.org/10.1007/s40430-017-0936-0).
- Zhang, Q., Yang, Z., Wang, C., Yang, Y. and Zhang, R. (2019a), "Intelligent control of active shock absorber for high-speed elevator car", *Proceedings of the Institution of Mechanical Engineers, Part C: Journal of Mechanical Engineering Science*, SAGE Publications, Vol. 233, pp. 3804-3815, doi: [10.1177/0954406218810045](https://doi.org/10.1177/0954406218810045).
- Zhang, R., Wang, C., Zhang, Q. and Liu, J. (2019b), "Response analysis of non-linear compound random vibration of a high-speed elevator", *Journal of Mechanical Science and Technology*, Vol. 33 No. 1, pp. 51-63, doi: [10.1007/s12206-018-1206-5](https://doi.org/10.1007/s12206-018-1206-5).

Corresponding author

Yaxing Ren can be contacted at: yaxing.ren@hotmail.com